A. KAPUŚCIŃSKA[1*], L. KWIATKOWSKI[1], P. WACH[1], A. MAZUREK[1], R. DIDUSZKO[2]

ANTICORROSION PROPERTIES AND MORPHOLOGY OF PHOSPHATE COATING FORMED ON NITRIDED SURFACE OF 42CrMo4 STEEL

The subject of the study concerns the enhancement of corrosion and wear resistance of nitrided 42CrMo4 steel by the formation of zinc phosphate top layer. The present work is aimed at the assessment of the effect of increasing thickness of nitrided layer from approximately 2 µm to 16 µm on the morphology and properties of zinc phosphate coating. XRD analysis showed that along with the increase in the thickness of the nitrides layer, a change in the phase composition was observed. SEM/EDS examination revealed that top layer consists of crystalline zinc phosphate coating. The shape and size of crystals does not significantly depend on a thickness of nitrides layer but corrosion resistance determined by potentiodynamic method in 0.5M NaCl increased with an increase of thickness of a "white layer". Similarly the wear resistance determined by the 3-cone-roll test was also the highest for 16 µm nitride layer.

Keywords: corrosion resistance, phosphating, gas nitriding, γ' nitrides, ε nitrides

1. Introduction

Nitriding processes are applied to the parts, for which high surface hardness, high corrosion resistance and resistance to wear is required [1-8]. The increased resistance to corrosion and wear by friction of nitrided layers depends on the properties of the substrate i.e. on the properties of a layer of iron nitrides. Adjustment of technological parameters of nitriding by using modern methods of the process control makes possible to form a surface layer of required thickness [9,10].

In order to provide acceptable corrosion resistance an additional post–treatment after nitriding process is usually is carried out i.e. oxidation and impregnation. These two steps prolong the production process and increase energy consumption. Oxidation is an additional heat treatment consisting of heating the product to a temperature of 530°C and withstanding in a steam for 2 hours with subsequent cooling in a furnace. Afterwards, an impregnation is carried out by immersing the product in oil or other medium containing corrosion inhibitors [11]. The operation is carried out at a temperature of about 60-80°C, followed by drying of elements that can last up to 24 hours. Therefore, it is interesting to introduce a technology that will provide at least comparable corrosion resistance of nitrided layers than those

obtained as a result of oxidation and impregnation. Potential candidates are passivation and / or phosphating processes.

The post-treatment of nitrided alloy steels involving passivation or phosphating with or without additional passivation was proposed by Flis et al. [12]. As a result of phosphating of plasma nitrided X10Cr18Ni9Ti steels, coatings with a thickness up to 10 µm were obtained. Corrosion resistance evaluated by electrochemical methods increased by an order of magnitude as long as the phosphate coating was passivated in a solution containing Cr (VI) or impregnated in oil. The influence of crystal size of the phosphate coating consisting of zinc and iron phosphates on the surface of X38CrMoV5-1 steel on corrosion resistance of the material was investigated in the work of Brojanowska et. al [13]. As in other works, the corrosion resistance of plasma-nitrided and phosphated steel was improved. Further improvement of corrosion resistance was obtained by an additional passivation/ sealing operation of the phosphate coating using benzaldoxime derivatives and organic solvents.

There could many of other possible solutions to seal nitride layers but one should consider the fact that phosphating is a topochemical reaction, which means that the properties of the coating are determined by the state of a substrate surface. Therefore the structure and surface composition of nitrided layer

[1]   INSTITUTE OF PRECISION MECHANICS, 3 DUCHNICKA STR., 01-796 WARSZAWA, POLAND
[2]   TELE AND RADIO RESEARCH INSTITUTE, 11 RATUSZOWA STR., 03-450 WARSZAWA, POLAND

*   Corresponding author: anna.kapuscinska@imp.edu.pl

seems to be a key factor to optimize the properties of a complex nitride/phosphate protective system. The present work is aimed at the assessment of the effect of increasing thickness of nitrided layer from approximately 0 to 16 μm along with the change in the phase composition of these layers on the morphology and corrosion properties of zinc phosphate top coating.

2. Experimental

The samples of 42CrMo4 steel which chemical composition is given in TABLE 1 were used in this study. Samples were subjected to standard heat treatment (hardening 850°C, tempering 600°C) and grinding in order to obtain the surface roughness $Ra = 0.32$ μm. After grinding the samples were gas nitrided to form the following types of nitride layers (nitriding process parameters are shown in Table 2):

I)   diffusion zone and a trace subsurface layer of iron nitrides – up to 2 μm (named Nd 2 μm),
II) diffusion zone and the subsurface layer of iron nitrides with a thickness of about 6÷8 μm (named Nd 8 μm),
III) diffusion zone and the subsurface layer of iron nitrides with a thickness of about 16÷18 μm (named Nd 16 μm).

Representative samples with a thickness of iron nitrides 2, 8 and 16 μm were used for further tests and are denoted in figures of the present paper as Nd 2 μm, Nd 8 μm and Nd 16 μm. The modern method of nitriding process control used in the Institute of Precision Mechanics makes possible to form the required thickness of the iron nitrides layer.

In the next step phosphating was carried out by chemical method in the solution containing 10 g/l Zn^{2+}, 11 g/l PO_4^{3-}, 14 g/l NO_3^-, at 50°C for 10 and 20 min.

XRD diffraction measurements were carried out by means of Siemens D500 diffractometer, equipped with a high-resolution semiconductor Si [Li] detector. This detector makes possible elimination of the fluorescent Fe radiation and $K\beta$ component of the Cu tube radiation. Operating parameters of radiation source: $U = 40$ kV, $I = 30$ mA. All patterns were measured in the 2 theta angle range 5-80°, with 0.05° steps and 4 seconds counting time per step. Phase composition analysis was performed using the ICDD PDF4 + 2018 database.

The microstructure of the produced layers was investigated using the Hitachi S-3400N scanning electron microscope with the Thermo Noran EDS analyzer.

Measurements of the current density – potential curves were carried out at room temperature in 0.5 M NaCl aerated solution at neutral pH. The exposed area of the sample surface was 0.28 cm^2.

Corrosion resistance was tested by means of potentiodynamic method. Current density – potential curves were recorded using three-electrode cell with the sample as the working electrode, platinum mesh and saturated calomel electrode (SCE) as counter and reference electrodes, respectively. The open circuit potential (OCP) was stabilized during 1 hour. After potential stabilization polarization curve was recorded in the potential range from –0.25 V vs. open circuit potential to positive values with scan rate of 1 mV/s. In order to distinguish between general and local type of corrosion a forward scan was reversed at a selected threshold at the intensive rise of a current density. Then a backward scan was recorded. If the backward scan is close to the course of the forward the dominant type of corrosion process is general corrosion. Significantly higher course of current densities for a backward scan indicates local type of corrosion i.e. pitting.

The measurements were carried out by means of Autolab system and the electrochemical corrosion parameters were estimated from the current-potential curves. I_{cor} and E_{cor} was calculated by the extrapolation of Tafel slopes using GPS software. All tests were repeated at least three times for each sample and the result represent an average course.

The wear resistance was determined by means of the friction test in three rollers-cone system (in accordance with PN-83/H-04302 Polish Standard) where the rotating counter-samples (cone) is pressed to three samples (rollers). The depth

TABLE 1

Chemical composition of 42CrMo4 (40 HM, 1.7225) steel

wt.%	C	Mn	Si	Cr	Mo	P	S	Ni	Cu
PN-EN 10083 1+A1:1999	0.38-0.45	0.40-0.70	0.17-0.37	0.80-1.10	0.15-0.25	max. 0.035	max. 0.035	max. 0.30	max. 0.30
Actual composition	0.40	0.42	0.26	1.02	0.17	0.01	0.007	0.04	0.05

TABLE 2

Technological parameters of nitriding process

Parameters of the nitriding process	Type I Nd 2 μm		Type II Nd 8 μm		Type III Nd 16 μm
	1st stage	2nd stage	1st stage	2nd stage	1st stage
Temperature, °C	460	500	490	540	560
Time, h	1	6	1	10	4
Process atmosphere composition	50% NH$_3$ – 50% NH$_{3diss}$	20% NH$_3$ – 80% NH$_{3diss}$	100% NH$_3$	45% NH$_3$ – 55% NH$_{3diss}$	100% NH$_3$
Nitriding potential*	5	0,5	17	1,8	3

* Nitriding potential N_p – is a parameter that controls and regulates the nitriding atmosphere. N_p determines the quotient of partial pressures NH$_3$ and H$_2$ in the atmosphere

of trace, which determines the linear wear, is estimated from measurements of ellipse diameter created by grooving the surface by each roll. Loading of 50 MPa unit pressures was applied in this work. Tests were carried out with drop lubrication at a rate of 30 drops of Lux-10 oil per minute. Three samples for each test were used.

3. Results and discussion

XRD analysis

Figure 1 presents the XRD diffractograms obtained for 42CrMo4 steel nitrided under technological conditions allowing the precise control of thickness of nitrides layer. Three different layers were obtained as the result of processes described in experimental part: Nd 2 µm, Nd 8 µm and Nd 16 µm.

The surface modified in process Nd 2 µm consists of a diffusion zone which is characterized by peaks corresponding to α-Fe (ICDD 6-696) and a layer of iron nitrides γ'-Fe_4N (ICDD 6-627). Formation of such phases is due to the low value of nitriding potential, resulting in less surface saturation by the nitrogen.

The layer of nitrides with a thickness of 8 micrometers obtained in process Nd 8 µm consists of γ'-Fe_4N and ε-Fe_3N (ICDD 49-1664) iron nitrides. The increase of the nitriding temperature and nitriding potential in the first and second stages of the process caused the formation of thicker nitrides layer and the formation of the ε-Fe_3N. This iron nitrides are characterized by a higher nitrogen content.

In the case of layer of nitrides with a thickness of 16 micrometers (process Nd 16 µm), in addition to γ'-Fe_4N and ε-Fe_3N nitrides, Fe_3O_4 (magnetite) (ICDD 19-629) was detected. High nitriding temperature in the process atmosphere of 100% ammonia and duration of 4 hours allowed to achieve the thickest nitrides layer. At the same time, the percentage of the Fe_3N phase increases. This fact is confirmed by the higher intensity of the peak responsible for the presence of iron nitrides Fe_3N.
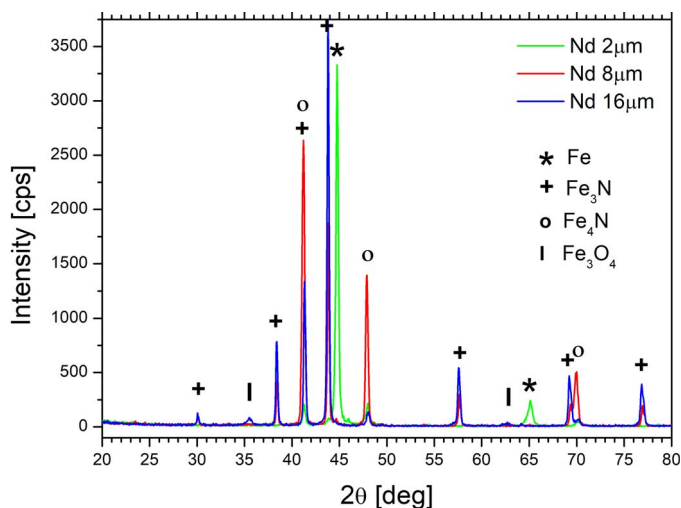
SEM/EDS examination

A complete phosphate coating with a characteristic shape of crystals is formed on each of tested nitrided substrates (Nd 2 µm, Nd 8 µm and Nd 16 µm). The shape of crystals is similar for all variants of the coating and forms needle-like crystals which in fact are plates crystallizing more or less perpendicularly to the substrate. The crystal size in particular coating is rather uniform, however it depends on the type of a substrate. A fine-size crystalline phosphate coating with a crystal size of approximately 5 µm was obtained on substrates having 8 µm and 16 µm thick layers of nitrides (Fig. 2b,c). Approximately 2 times larger crystals
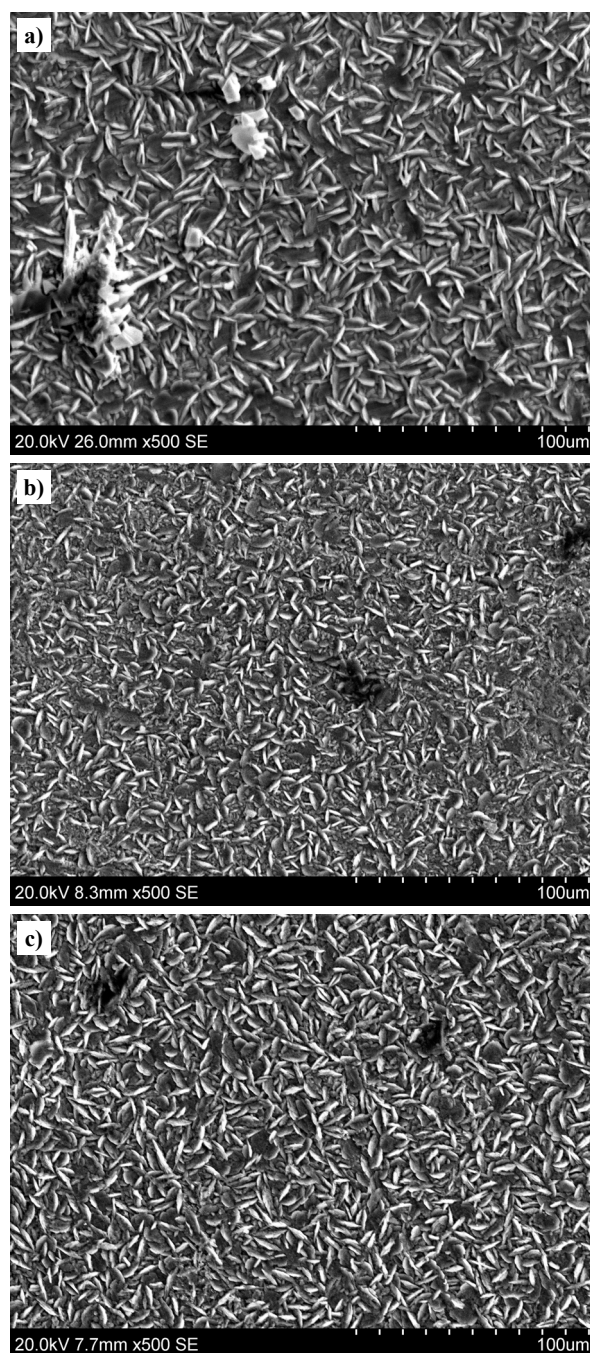

Fig. 2. SEM images of the phosphated (during 10 min.) samples obtained on the nitrided substrate containing layer of nitrides with a thickness of 2 µm (a), 8 µm (b) and 16 µm (c)

Fig. 1. X-ray diffraction pattern of 42CrMo4 steel after gas nitriding according to variant Nd 2 µm, Nd 8 µm and Nd 16 µm

grow on the surface with a trace layer of iron nitrides Nd 2 μm (Fig. 2a). The uniformity of the coating is disturbed by numerous crystal accretions, which presence is difficult to explain at this stage of the study but one can assume that excessive nucleation may occur on local agglomerates of γ'-Fe$_4$N. The elemental composition of the coatings for both times of phosphating (10 and 20 minutes) is similar and contains the components of the coating such us Zn, P, O as well as the substrates: Fe, N and Cr
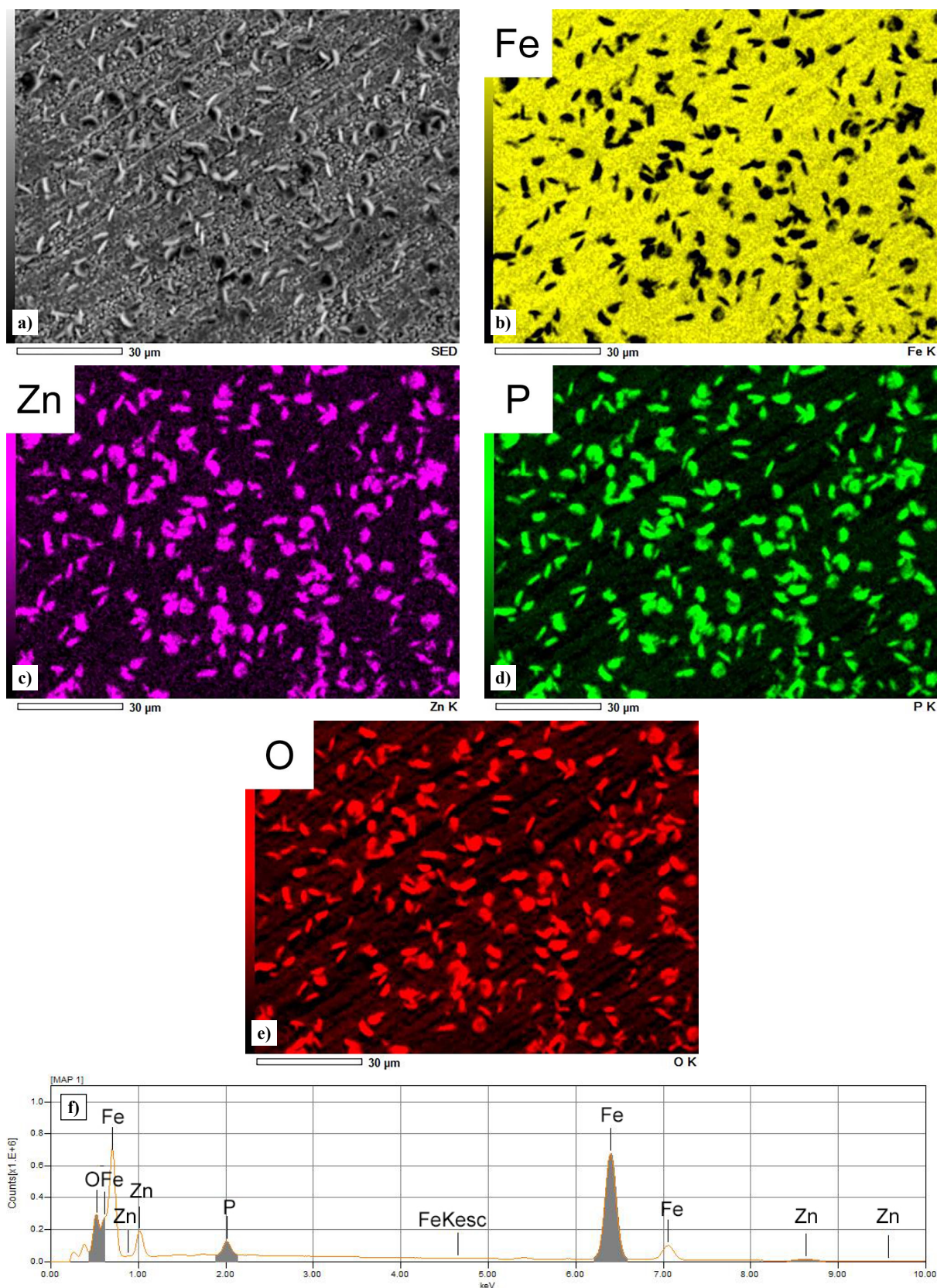

Fig. 3. SEM image (a) and EDS mapping of composition of Nd 16 μm sample after phosphating during 5 seconds: (b) the EDS mapping of element Fe, (c), (d) and (e) EDS mapping of elements Zn, P and O respectively, (f) EDS element analysis

(Table 3). This composition is typical for phosphate coatings obtained from solution with high content of zinc. Energy dispersive spectroscopy is effective only for materials containing heavy elements therefore these results should be considered qualitatively. As it is seen in Fig. 3 the nitrided substrate –variant Nd 16 µm – the nucleation of crystals takes place in the first seconds of the phosphating process. After five seconds, single crystals containing Zn, P and O were observed. It can be concluded that the nitrided substrate promotes nucleation and the formation of a phosphate conversion coating.

TABLE 3

EDS elemental analysis of Nd 2 µm + Ph 10 min, Nd 8 µm + Ph 10 min and Nd 16 µm + Ph 10 min

% atom.	Nd 2 µm + Ph 10 min	Nd 8 µm + Ph 10 min	Nd 16 µm + Ph 10 min
N	21.31	29.98	29.95
O	50.19	34.72	34.83
Na	9.12	3.81	4.27
P	5.06	1.89	2.09
C	—	18.77	19.88
Cr	0.20	0.12	0.10
Fe	9.86	8.86	6.82
Zn	4.26	1.74	2.07

Corrosion resistance

The effect of thickness and chemical content of nitrided surface of 42CrMo4 steel with or without phosphate coating on corrosion behaviour of samples immersed in 0.5 M NaCl solution is shown in Fig. 4-6 and Table 3.

In the case of the phosphate coating formed on the surface of diffusion layer, a significant increase in corrosion resistance was obtained in comparison with non phosphated surface (Fig. 4). The value of corrosion potential after phosphating is about 0.2 V more positive, and the corrosion current density is

TABLE 4

Electrochemical parameters determined from polarization curves

	E_{cor}, V	I_{cor}, A/cm^2	E_{pit}, V	I_{pas}, A/cm^2
heat treatment + Nd 2 µm	−0.78	$1.6 \cdot 10^{-6}$	—	—
heat treatment + Nd 2 µm + Ph 10 min.	−0.57	$2.3 \cdot 10^{-6}$	—	—
heat treatment + Nd 2 µm + Ph 20 min.	−0.57	$1.3 \cdot 10^{-6}$	—	—
heat treatment + Nd 8 µm	−0.39	—	0.12	$3.1 \cdot 10^{-6}$
heat treatment + Nd 8 µm + Ph 10 min.	−0.44	—	0.12	$1.7 \cdot 10^{-6}$
heat treatment + Nd 8 µm + Ph 20 min.	−0.51	—	0.12	$1.1 \cdot 10^{-6}$
heat treatment + Nd 16 µm	−0.85	—	1.20	$4.8 \cdot 10^{-4}$
heat treatment + Nd 16 µm + Ph 10 min.	−0.79	—	0.95	$6.7 \cdot 10^{-5}$
heat treatment + Nd 16 µm + Ph 20 min.	−0.80	—	0.95	$4.8 \cdot 10^{-5}$

lower by an order of magnitude. Corrosion process is controlled by cathodic reaction of the oxygen depolarisation which is typical for the mechanism of general corrosion. In addition, the same slope of both cathodic and anodic polarization curves in presence and absence of the phosphate coating indicate quite clearly that the protection of substrate by the coating relies upon a significant reduction in the surface area available for cathodic reactions taking place on a substrate. The influence of the phosphating time is not critical here. Slightly better corrosion resistance for the coating formed during 10 min. of phosphating is obtained.

If the phosphating process is carried out on a nitrided layer containing iron nitrides of a thickness of 8 µm, the increase of corrosion resistance is observed and the control of the corrosion rate changes from the cathodic reaction to the anodic (Fig. 5b) leading in this case to mixed control conditions. It should be noted that the increase of the current density at the potential of +0.1 to +0.2 V is related to occurrence of local corrosion.
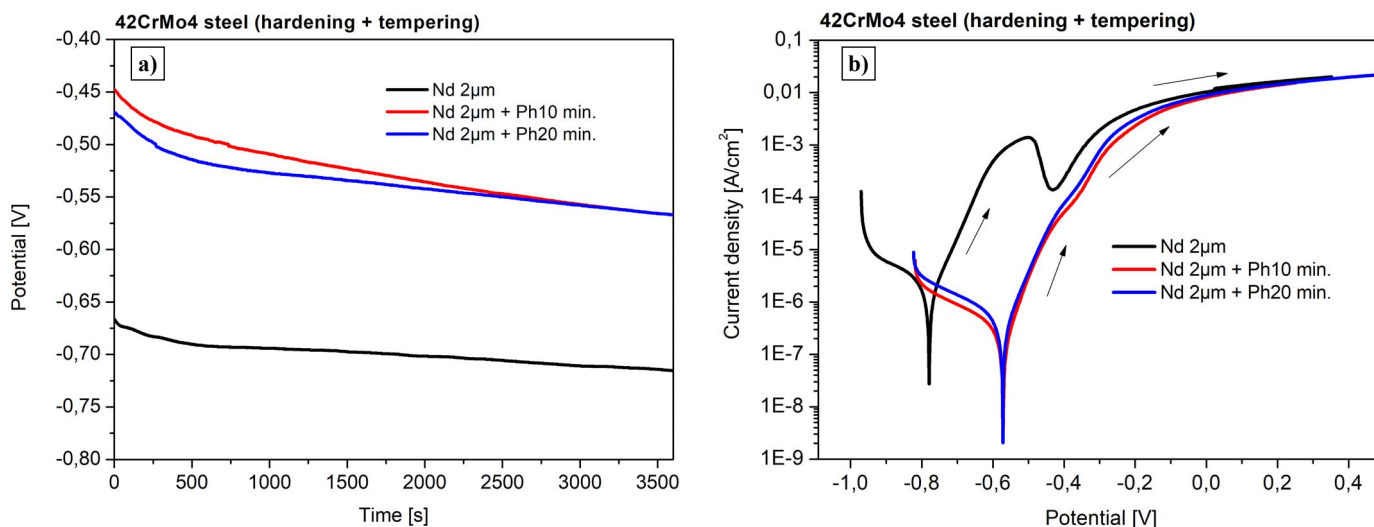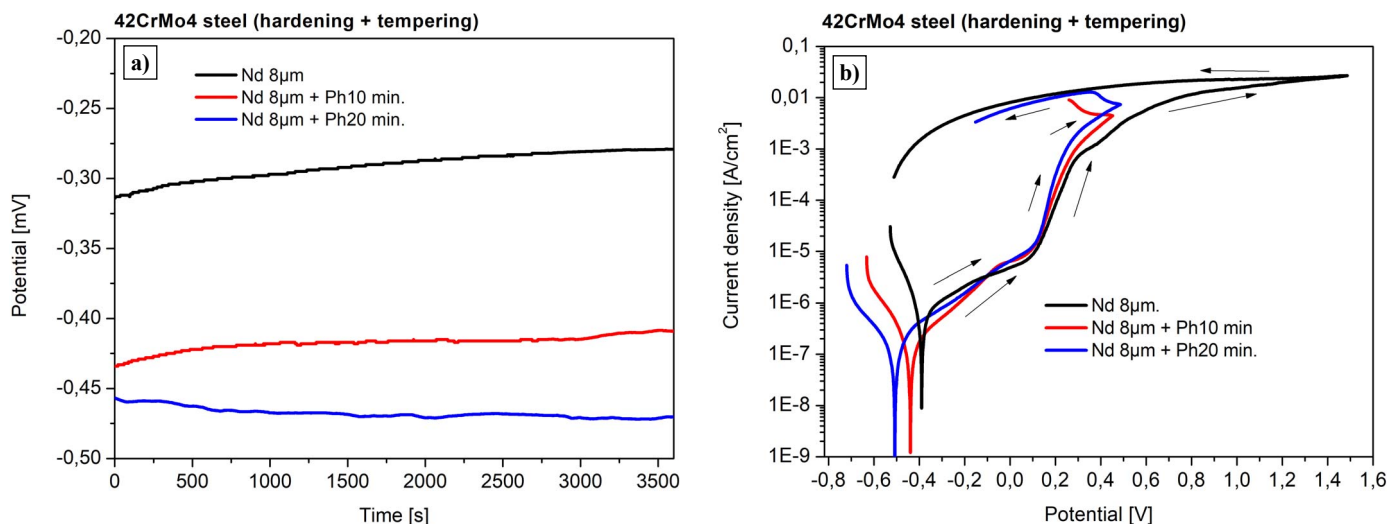

Fig. 4. A course of an open circuit potential a) and polarization curves b) determined after 1 hour of immersion in 0,5 M NaCl for samples of 42CrMo4 nitrided steel (nitrided layer 2 µm) and after 10 min. and 20 min. of phosphating

476

Fig. 5. A course of an open circuit potential a) and polarization curves b) determined after 1 hour of immersion in 0,5 M NaCl for samples of 42CrMo4 nitrided steel (nitrided layer 8 μm) and after 10 min. and 20 min. of phosphating
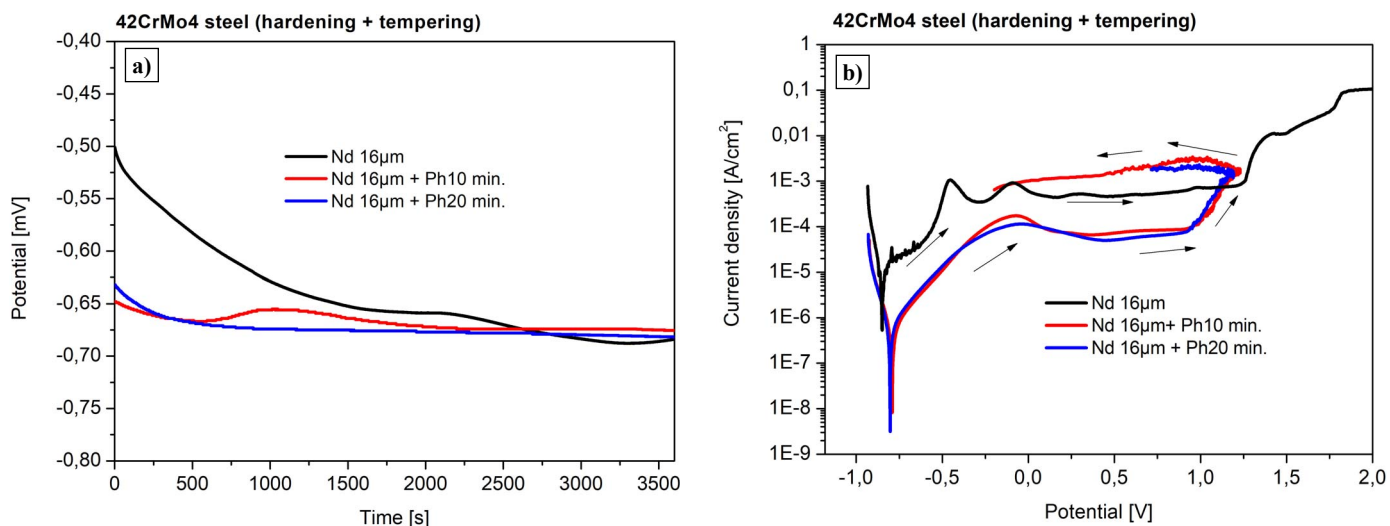

Fig. 6. A course of an open circuit potential a) and polarization curves b) determined after 1 hour of immersion in 0,5 M NaCl for samples of 42CrMo4 nitrided steel (nitrided layer 16 μm) and after 10 min. and 20 min. of phosphating

Determination of corrosion currents in this case by the Tafel extrapolation method is no longer appropriate, because this method is limited to the case of activation control of the corrosion process.

Decrease a susceptibility to local corrosion for the 16 μm thick nitrides layer is observed, while the general corrosion resistance remains unchanged (Fig. 6). The phosphate coating substantially limits the course of corrosion reactions of the substrate (2 maxima on the curve for nitriding in Fig. 6b), but the current density in the passive range indicates the moderate protective properties of this layer. However, the layer is stable in a wide range of potentials from +0.4 V to approx. +1.0 V. After exceeding the 1.0 V potential, the current density increases intensively due to local corrosion. This is indicated by the backward polarization curve at higher current densities. The presence of Fe_3O_4 as a component of the nitrided layer may be responsible for stabilization of the passive range.

The polarization curves recorded for nitrided steel are characterized by the presence of peaks in the anodic region. In the case of the Nd 2 μm variant, the characteristic peak was observed at potential of approximately –0.4 V (Fig. 4b) for Nd 8 μm a kind of inflection point at –0.14 V (Fig. 5b) whereas for Nd 16 μm at –0.45 V and –0.10 V (Fig. 6b). Mańkowski conducted comparative polarization measurements for Armco and 38HMJ steel nitrided under the same conditions, where γ'-Fe_4N, ε-$Fe_{2-3}N$ phase were obtained [14]. He suggested that the maxima observed in the case of nitrided 38HMJ steel are related to anodic dissolution of steel and various nitride forms: γ'-Fe_4N, ε-$Fe_{2-3}N$. Other authors proved that in neutral 0.05 M NaCl, the corrosion potentials of the Fe_4N and $Fe_{2-3}N$ phases are -0.52 and -0.25 V respectively, [15]. Therefore it can be concluded that similar phenomena i.e. anodic iron dissolution followed by subsequent reaction of iron nitrides may occur. More detailed studies are necessary in order to assign reaction of specific phases to particular anodic peaks.